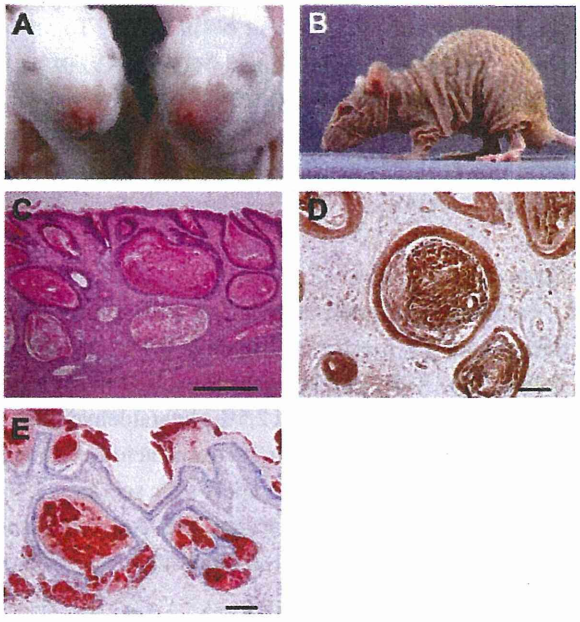

Fig. 1. Phenotypic and morphological characteristics of the Kyoto rhino rat. A: Right; a 2-week-old *krh/krh* rat with characteristic hair loss on the snout. Left; a littermate *krh/+* rat. B: Rhinocerotic appearance of a 10-week-old *krh/krh* rat. C: Histopathology of 9-week-old *krh/krh* rat skin. HE staining. Bar=500 μm. D: IHC of keratin of a 9-week-old *krh/krh* rat. Bar=100 μm. E: Oil Red O staining of a 17-week-old *krh/krh* rat. Bar=100 μm.

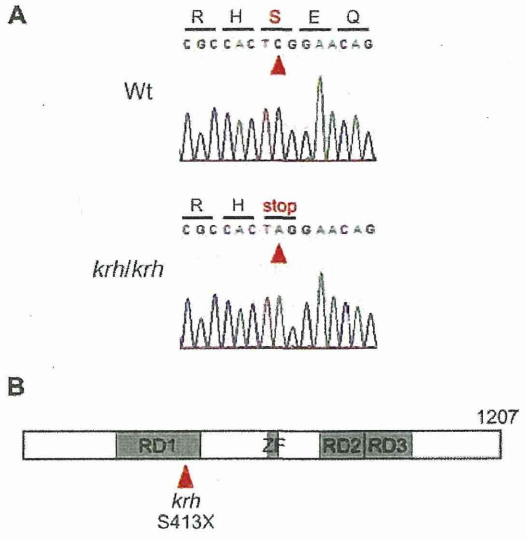

Fig. 2. Identification of the *krh* mutation. A: Results of direct sequencing of *Hr* cDNA of wild-type and *krh/krh* rats. The C-to-A nonsense mutation at position 1,238 is indicated by red arrowheads. The substitution produces a stop codon at amino acid residue 413 of protein HR. B: Schematic of the conserved domains in rat protein HR. RD1, RD2, and RD3 are used to denote the repression domains and ZF is used to denote the zinc-finger domain. The mutation site Ser413Ter is noted with a red arrowhead.

surface of the epidermis (Fig. 1E). These findings are indicators that the *krh/krh* skin and hair phenotypes are similar to those of *rh* at the *Hr* locus of the laboratory mouse [7].

krh is an Hr nonsense mutation

Hr on Chr 15 was believed to be the best candidate for *krh* and therefore the genotype of the backcross progeny was determined using genetic markers for Chr 15. We obtained 12 *krh/krh* and 8 *krh/+* rats from the (BN/SsNSlc × F344-*krh/krh*)F_1 × F344-*krh/krh* backcross. A significant linkage relationship was observed between *krh* and *D15Rat10* (42.7 Mb) with no recombination (χ^2=21.6, P<0.01), which is indicative that *krh* is located <13.9 cM away from *D15Rat10* with 95% probability [11]. *krh* was expected to span from 28.8 Mb to 56.6 Mb of Chr 15, within which the *Hr* locus (50.9 Mb) was mapped (RGSC v3.4).

Sequencing analyses of *Hr* cDNA obtained from *krh/krh* skin samples revealed that adenine (A) had been substituted for cytosine (C) at nucleotide position 1,238 from the start of the CDS (c. 1,238 C>A). This substitution resulted in a stop codon at amino acid 413 of the HR protein (p. Ser413Ter) (Fig. 2A). The truncated HR protein lacked a zinc-finger domain, a part of repression domain (RD) 1, and all of RD2 and RD3 (Fig. 2B). We characterized *krh* as an *Hr* nonsense mutation and called it Hr^{krh}.

Focal glomerulosclerosis and proteinuria in the aged Hr^{krh}/Hr^{krh} rat

Histopathological examinations of organs that were taken from Hr^{krh}/Hr^{krh} rats at 40 weeks of age were performed. No lesions that are associated with autoimmune diseases were observed, however, prominent glomerular lesions were noted in the kidneys of the Hr^{krh}/Hr^{krh} rats. These lesions were focal lesions that had collapsed glomeruli and protein exudates in Bowman capsule and the renal tubules (Fig. 3A and 3C), and segmental prolifera-

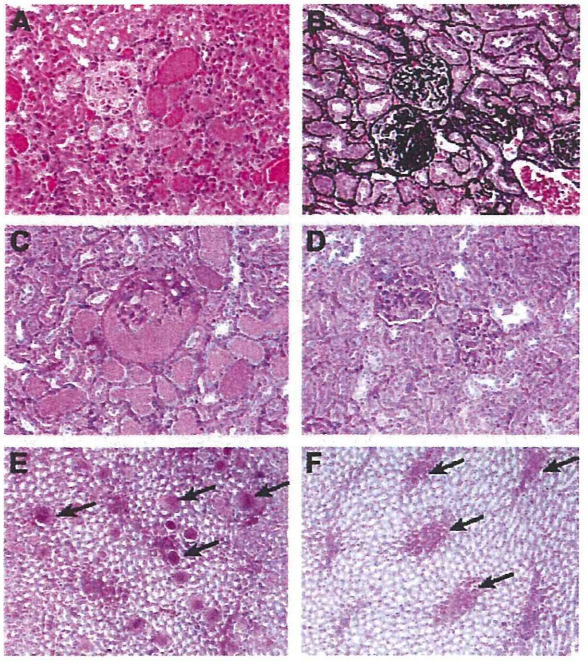

Fig. 3. Focal glomerular sclerotic lesions in 40-week-old Hr^{krh}/Hr^{krh} rat. Note that a collapsed glomerulus with protein exudates in Bowman's capsule and protein casts in renal tubules (A, C), and segmental proliferation of mesangial matrices (B, D) were seen. In the renal medulla, protein casts were notable in the collecting tubules (E) (arrows), but those in a wild-type F344 rat (+/+) were limited only to Henle's loop (F) (arrows). A: HE; B: PAM; C–F: PAS staining.

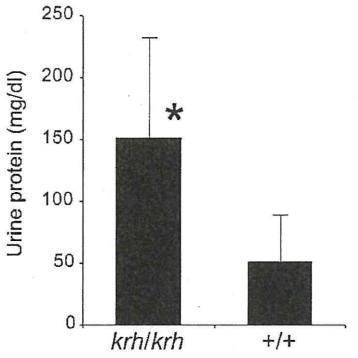

Fig. 4. Urine protein concentrations of Hr^{krh}/Hr^{krh} rats and wild-type F344 (+/+) rats. The Hr^{krh} homozygous rats had significantly higher urine protein concentrations than age-matched wild-type rats. Bars indicate standard deviation. *: $P<0.02$.

tion of the mesangial matrices (Fig. 3B and 3D). There was no inflammatory cell infiltration into the glomeruli and interstitium. In the renal medulla, protein casts were notably present in the collecting tubules (Fig. 3E). For the wild-type rats, protein casts were only observed in Henle's loop, possibly due to the effects of aging (Fig. 3F). These findings are indicators that the lesions that were observed in the F344-Hr^{krh}/Hr^{krh} rat were caused by focal glomerulosclerosis (FGS). Moreover, Hr^{krh}/Hr^{krh} rats at 40 weeks of age had proteinuria. The Hr^{krh} homozygous rats had significantly higher urine protein concentrations than age-matched wild-type rats: 152 ± 80.3 vs. 51.0 ± 38.5 mg/dl, (average ± SD), $P<0.02$ (Fig. 4).

From the electron microscopic observations, the segmental glomerular sclerotic lesions were characterized as having proliferating mesangial matrices (Fig. 5A). The proliferation was associated with the dendritic processes of mesangial cells and on rare occasions with dense deposits in the mesangial regions. Foot process fusion was often observed in these glomeruli (Fig. 5B).

Discussion

The *krh* mutation was identified as an *Hr* nonsense mutation and therefore called Hr^{krh}. Protein HR is a nuclear receptor co-repressor for multiple nuclear receptors, such as the thyroid hormone receptor and the vitamin D receptor [23]. In the hair follicle (HF), the absence of functioning HR proteins results in the synthesis of premature and dysregulated catagen. This results in the destruction of the normal HF architecture and abrogates the HF's ability to cycle [20]. The Hr^{krh}/Hr^{krh} rat has cystic hair follicles and suffers from a premature hair cycle (Fig. 1). The truncated HR protein that is encoded by the Hr^{krh} nonsense mutation is caused by a lack of functional domains which play important roles in regulating target genes [23]. Additionally, the mutation may cause nonsense mediated mRNA decay. Therefore, it is likely that Hr^{krh} may be a loss-of-function mutation. In humans, *HR* mutations are associated with congenital alopecia, such as ALUNC and APL [2, 4, 9]. Because rats are suitably sized for handling and manipulating [5, 21], the Hr^{krh}/Hr^{krh} rat may be a useful animal model for developing therapies for these human diseases.

The aged Hr^{krh} homozygous rat has FGS which is as-

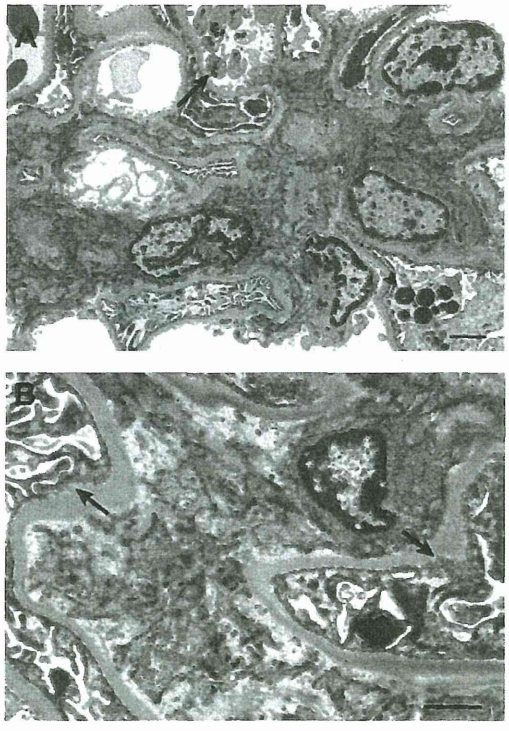

Fig. 5. Fine structures of glomerular lesions in the Hr^{krh}/Hr^{krh} rat. A: Proliferative lesions of mesangial matrices associated with significant dendritic projections from mesangial cells. Platelet aggregation was observed in a capillary loop (arrow). Intracellular hyaline droplets were significant in a podocyte (arrowhead). B: Foot process fusion (arrows) and a proliferative lesion of mesangial matrices that was not associated with dense deposits in mesangial regions and the glomerular basement membrane. Bar: 2 μm.

sociated with severe proteinuria. FGS is a descriptor for a pathological finding in the kidneys. When a nephritic range of proteinuria is observed, patients are diagnosed as having focal segmental glomerulosclerosis (FSGS). FSGS is classified by morphological variants including collapsed glomeruli, cellular proliferation, tip lesions, and diffuse mesangial proliferation [10]. The lesions that were observed in the F344-Hr^{krh} rat are characteristic of collapsed glomeruli associated with protein exudates in Bowman's capsule and may involve a collapsed variant of FSGS. Thus, the F344-Hr^{krh} rat may have potential as a model of nephritic FSGS.

FGS has not been reported for the APL or ALUNC family, and *Hr*-mutant mice, [2, 3, 7]. It is believed that FGS has a heterogeneous etiology and that it may manifest through multiple genetic factors [10]. The F344-Hr^{krh} rats were derived by employing ENU mutagenesis. The founder animals (G_1 generation) were expected to carry no more than four ENU-induced mutations in their CDS, if the CDS occupies 1% of the genome [16]. The F344-Hr^{krh} rats were mated by inbreeding without backcrossing to F344 rats to eliminate ENU-induced mutations other than the Hr^{krh} mutation. Thus, it is likely that the F344-Hr^{krh} rat may harbor mutation(s) that may play a role in the pathogenesis of FGS. FGS in Hr^{krh}/Hr^{krh} rats might be caused by unidentified mutation(s) that were induced by ENU or the combined effects of such mutation(s) with the Hr^{krh} mutation.

The Hr^{rh}/Hr^{rh} mouse has the nonsense mutation (R597X) [8] and develops hypergammaglobulinemia. The excess immunoglobulins that are produced due to this disease are deposited in the basement membranes of the skin, spleen, liver, and kidney, and antinuclear antibodies are produced. These symptoms appear in young mice and increase in severity with age [14]. Although the F344-Hr^{krh}/Hr^{krh} rat has a nonsense mutation (S413X), the mutation is not associated with an autoimmune disease or IgM, IgG, and C3 deposition in the kidneys (data not shown). Generally, pathological phenotypes that are associated with this disease are often influenced by a predisposed genetic background [18, 19]. Therefore, genes that are predisposed to causing autoimmune diseases in *rh/rh* mice may be absent in F344-Hr^{krh} rats. By replacing the genetic background of F344-Hr^{krh} with those of other rat strains, we might find autoimmune disease in Hr^{krh}/Hr^{krh} rats.

In summary, a novel rat mutant strain, F344-Hr^{krh}, was established that carries an *Hr* nonsense mutation (S413X). In addition to the hair loss phenotype, Hr^{krh} homozygous rats suffer from proteinuria and FGS. Therefore, F344-Hr^{krh} may have potential as a model of skin disease as well as nephritic FSGS.

Acknowledgments

This work was supported in part by Grants-in-aid for Scientific Research from the Japan Society for the Promotion of Science (21300153 to TK) and a Grant-in-aid for Cancer Research from the Ministry of Health, Labour

and Welfare. We are grateful to M. Yokoe, M. Terada, N. Takahira, and M. Sudo for their excellent technical assistance. Rat strain F344-*Hr*^{krh} (NBRP Rat No: 0471) is deposited in the National BioResource Project-Rat.

References

1. Ahearn, K., Akkouris, G., Berry, P.R., Chrissluis, R.R., Crooks, I.M., Dull, A.K., Grable, S., Jeruzal, J., Lanza, J., Lavoie, C., Maloney, R.A., Pitruzzello, M., Sharma, R., Stoklasek, T.A., Tweeddale, J., and King, T.R. 2002. The Charles River "hairless" rat mutation maps to chromosome 1: allelic with fuzzy and a likely orthologue of mouse frizzy. *J. Hered.* 93: 210–213.
2. Ahmad, W., Faiyaz ul Haque, M., Brancolini, V., Tsou, H.C., ul Haque, S., Lam, H., Aita, V.M., Owen, J., deBlaquiere, M., Frank, J., Cserhalmi-Friedman, P.B., Leask, A., McGrath, J.A., Peacocke, M., Ahmad, M., Ott, J., and Christiano, A.M. 1998. Alopecia universalis associated with a mutation in the human hairless gene. *Science* 279: 720–724.
3. Ahmad, W., Ratterree, M.S., Panteleyev, A.A., Aita, V.M., Sundberg, J.P., and Christiano, A.M. 2002. Atrichia with papular lesions resulting from mutations in the rhesus macaque (*Macaca mulatta*) hairless gene. *Lab. Anim.* 36: 61–67.
4. Ahmad, W., Zlotogorski, A., Panteleyev, A.A., Lam, H., Ahmad, M., ul Haque, M.F., Abdallah, H.M., Dragan, L., and Christiano, A.M. 1999. Genomic organization of the human hairless gene (*HR*) and identification of a mutation underlying congenital atrichia in an Arab Palestinian family. *Genomics* 56: 141–148.
5. Aitman, T.J., Critser, J.K., Cuppen, E., Dominiczak, A., Fernandez-Suarez, X.M., Flint, J., Gauguier, D., Geurts, A.M., Gould, M., Harris, P.C., Holmdahl, R., Hubner, N., Izsvak, Z., Jacob, H.J., Kuramoto, T., Kwitek, A.E., Marrone, A., Mashimo, T., Moreno, C., Mullins, J., Mullins, L., Olsson, T., Pravenec, M., Riley, L., Saar, K., Serikawa, T., Shull, J.D., Szpirer, C., Twigger, S.N., Voigt, B., and Worley, K. 2008. Progress and prospects in rat genetics: a community view. *Nat. Genet.* 40: 516–522.
6. Bazzi, H., Kljuic, A., Christiano, A.M., and Panteleyev, A.A. 2004. Intragenic deletion in the Desmoglein 4 gene underlies the skin phenotype in the Iffa Credo "hairless" rat. *Differentiation* 72: 450–464.
7. Bult, C.J., Eppig, J.T., Kadin, J.A., Richardson, J.E., and Blake, J.A. 2008. The Mouse Genome Database (MGD): mouse biology and model systems. *Nucleic Acids Res.* 36: D724–728.
8. Cachon-Gonzalez, M.B., San-Jose, I., Cano, A., Vega, J.A., Garcia, N., Freeman, T., Schimmang, T., and Stoye, J.P. 1999. The hairless gene of the mouse: relationship of phenotypic effects with expression profile and genotype. *Dev. Dyn.* 216: 113–126.
9. Cichon, S., Anker, M., Vogt, I.R., Rohleder, H., Putzstuck, M., Hillmer, A., Farooq, S.A., Al-Dhafri, K.S., Ahmad, M., Haque, S., Rietschel, M., Propping, P., Kruse, R., and Nothen, M.M. 1998. Cloning, genomic organization, alternative transcripts and mutational analysis of the gene responsible for autosomal recessive universal congenital alopecia. *Hum. Mol. Genet.* 7: 1671–1679.
10. Dagati, V. 1994. The many masks of focal segmental glomerulosclerosis. *Kid. Int.* 46: 1223–1241.
11. Friedman, J.M., Leibel, R.L., and Bahary, N. 1991. Molecular mapping of obesity genes. *Mamm. Genome* 1: 130–144.
12. Inazu, M. and Sakaguchi, T. 1984. Morphologic characteristics of the skin of bald mutant rats. *Lab. Anim. Sci.* 34: 584–587.
13. Ishii, Y., Tsutsui, S., Doi, K., and Itagaki, S. 1997. Hair follicles of young Wistar strain hairless rats: a histological study. *J. Anat.* 191: 99–106.
14. Kawaji, H., Tsukuda, R., and Nakaguchi, T. 1980. Immunopathology of rhino mouse, an autosomal recessive mutant with murine lupus-like disease. *Acta Pathol. Jpn.* 30: 515–530.
15. Kuramoto, T., Kitada, K., Inui, T., Sasaki, Y., Ito, K., Hase, T., Kawagachi, S., Ogawa, Y., Nakao, K., Barsh, G.S., Nagao, M., Ushijima, T., and Serikawa, T. 2001. Attractin/mahogany/zitter plays a critical role in myelination of the central nervous system. *Proc. Natl. Acad. Sci. U.S.A.* 98: 559–564.
16. Mashimo, T., Yanagihara, K., Tokuda, S., Voigt, B., Takizawa, A., Nakajima, R., Kato, M., Hirabayashi, M., Kuramoto, T., and Serikawa, T. 2008. An ENU-induced mutant archive for gene targeting in rats. *Nat. Genet.* 40: 514–515.
17. Nanashima, N., Akita, M., Yamada, T., Shimizu, T., Nakano, H., Fan, Y., and Tsuchida, S. 2008. The hairless phenotype of the Hirosaki hairless rat is due to the deletion of an 80-kb genomic DNA containing five basic keratin genes. *J. Biol. Chem.* 283: 16868–16875.
18. Nose, M. 2007. A proposal concept of a polygene network in systemic vasculitis: lessons from MRL mouse models. *Allergol. Int.* 56: 79–86.
19. Nose, M., Nishimura, M., and Kyogoku, M. 1989. Analysis of granulomatous arteritis in MRL/Mp autoimmune disease mice bearing lymphoproliferative genes. The use of mouse genetics to dissociate the development of arteritis and glomerulonephritis. *Am. J. Pathol.* 135: 271–280.
20. Panteleyev, A.A., Botchkareva, N.V., Sundberg, J.P., Christiano, A.M., and Paus, R. 1999. The role of the hairless (*hr*) gene in the regulation of hair follicle catagen transformation. *Am. J. Pathol.* 155: 159–171.
21. Serikawa, T., Mashimo, T., Takizawa, A., Okajima, R., Maedomari, N., Kumafuji, K., Takami, F., Neoda, Y., Otsuki, M., Nakanishi, S., Yamasaki, K., Voigt, B., and Kuramoto, T. 2009. National BioResource Project-Rat and related activities. *Exp. Anim.* 58: 333–341.
22. Sun, J., Silva, K.A., McElwee, K.J., King, L.E., and Sundberg, J.P. 2008. The C3H/HeJ mouse and DEBR rat models for alopecia areata: review of preclinical drug screening approaches and results. *Exp. Dermatol.* 17: 793–805.
23. Thompson, C.C., Sisk, J.M., and Beaudoin, G.M. 3rd. 2006. Hairless and Wnt signaling: allies in epithelial stem cell differentiation. *Cell Cycle* 5: 1913–1917.

Exp. Anim. 59(2), 147–155, 2010

—Original—

Genetic Analyses of Fancy Rat-Derived Mutations

Takashi KURAMOTO, Mayuko YOKOE, Kayoko YAGASAKI, Tatsuya KAWAGUCHI, Kenta KUMAFUJI, and Tadao SERIKAWA

Institute of Laboratory Animals, Graduate School of Medicine, Kyoto University, Yoshidakonoe-cho, Sakyo-ku, Kyoto 606-8501, Japan

Abstract: To collect rat mutations and increase the value of the rat model system, we introduced fancy-derived mutations to the laboratory and carried out genetic analyses. Six fancy rats were shipped from a fancy rat colony in the USA and used as founders. After initial crosses with a laboratory strain, TM/Kyo or PVG/Seac, inbreeding started and 6 partially inbred lines, including 2 sublines, were produced as Kyoto Fancy Rat Stock (KFRS) strains. During inbreeding, we isolated 9 mutations: 5 coat colors, American mink (*am*), Black eye (*Be*), grey (*g*), Pearl (*Pel*), siamese (*sia*); 1 coat pattern, head spot (*hs*); 2 coat textures, Rex (*Re*), satin (*sat*); and an ear pinnae malformation, dumbo (*dmbo*). Genetic analyses mapped 7 mutations to particular regions of the rat chromosomes (Chr): *am* to Chr 1, *sia* to Chr 1, *sat* to Chr 3, *Re* to Chr 7, *g* to Chr 8, *dmbo* to Chr 14, and *hs* to Chr 15. Candidate gene analysis revealed that a missense mutation in the tyrosinase gene, Ser79Pro, was responsible for *sia*. From mutant phenotypes and mapping positions, it is likely that all mutations isolated in this study were unique to the fancy rat. These findings suggest that fancy rat colonies are a good source for collecting rat mutations. The fancy-derived mutations, made available to biomedical research in the current study, will increase the scientific value of laboratory rats.

Key words: bioresource, coat color, genetic mapping, inbreeding, mutation

Introduction

Genetic analyses of common diseases in humans have revealed that gene mutations are involved in diseases. Genome sequencing projects of various mammalian species followed by comparative genome analyses have revealed that a large number of genes are shared among species. Thus, it is thought that mutations found in model animals and animals carrying such mutations can contribute to the better understanding of human diseases.

The laboratory rat (*Rattus norvegicus*) has been widely used as an animal model of human diseases, because its size is suitable for manipulation [1, 27]. Sequencing of the rat genome has shown that the rat has about 20,000 predicted genes and shares as many as 90% with humans [9]. So far, at least 70 mutations have been identified as causative genes of specific diseases and rat strains carrying such mutations can be used as good animal models for these diseases; however, considering the high number of rat genes predicted [9], more mutations will be required to investigate the full range of diseases. Thus,

(Received 25 August 2009 / Accepted 22 October 2009)

Address corresponding: T. Kuramoto, Institute of Laboratory Animals, Graduate School of Medicine, Kyoto University, Yoshidakonoe-cho, Sakyo-ku, Kyoto 606-8501, Japan

collecting rat mutations and making rats carrying these mutations available as bioresources would enhance the scientific value of rats as an animal model for human diseases.

There are several approaches to collecting rat mutations. They include discovering naturally occurring mutations and inducing mutations by random mutagenesis [21]. In addition, attempts have been made to collect mutations outside of the laboratory, from the field or fancy rat colonies; indeed, some inbred strains have been established from wild captured rats [11]. However, fancy rats have not been surveyed as a source of mutations, with a few exceptions [26].

Fancy rat colonies have potential as a source for collecting novel rat mutations, because various mutations are considered to persist only in fancy rats, largely coat and eye color mutations, and coat pattern mutations. Thus, when they are available in laboratory rats, most will provide opportunities to study the function of melanocytes, which are not only responsible for pigment synthesis in the skin and hair, but are also involved in inner ear and eye functions [30]. In addition, in human, dysfunctions of melanocytes result in skin disorders such as oculocutaneous albinism, piebaldism and skin cancers [12, 29], prompting us to introduce mutations found in the current fancy rat colonies to the laboratory and establish them as novel bioresources available for biomedical research.

In this study, we imported 6 fancy rats from a fancy rat colony in the USA to our laboratory. We tried to isolate fancy mutations and establish inbred strains carrying them. During inbreeding, we isolated 9 mutations, of which 7 were mapped to particular genomic regions of rat chromosomes. A coat color mutation, siamese, was identified as a missense mutation in the rat tyrosinase gene.

Materials and Methods

Animals

In July, 2005, 6 fancy rats were imported from a fancy rat colony named Spoiled Ratten Rattery (SRR) kept by Ms. E. Brooks in Kansas City, Missouri, USA (http://www.spoiledratten.com/index.html). These rats (SRR01-06) were used as founders to establish fancy-derived strains. SRR01 was female and the others were males. It was known that these founders carried the following mutations (Table 1): SRR01 carried dumbo (*dmbo*), Rex (*Re*), and satin (*sat*); SRR02 carried *sat* and siamese (*sia*); SRR03 carried American mink (*am*), grey (*g*), and Pearl (*Pel*); SRR04 carried dumbo (*dmbo*); SRR05 carried *Re*; and SRR06 carried Black eye (*Be*). TM/Kyo and PVG/Seac rats were selected as mating partners to obtain progeny from the founder fancy rats, because they are homozygous for nonagouti (*a/a*) and hooded (*h/h*) recessive mutations. SRR01, SRR05, and SRR06 were crossed with the TM/Kyo strain and SRR02, SRR03, and SRR04 were crossed with the PVG/Seac strain. Following caesarean operations, F_1 hybrids were introduced to specific pathogen-free (SPF) facilities in our institute. Brother-sister mating was carried out to establish fancy rat-derived strains for each founder. At each generation during inbreeding, rats showing the mutant phenotypes were selected. When different mutant phenotypes were found in an inbreeding line, sublines were separated.

To map the mutations isolated from fancy rats, a male rat representing each strain was used to make F_1 hybrids with BN/SsNSlc (BN) or WTC/Kyo (WTC) female rats.

Animal care and experimental procedures were approved by the Animal Research Committee, Kyoto University and were conducted according to the Regulation on Animal Experimentation at Kyoto University.

Genetic mapping

To map *sat* and *sia* mutations, SRR02 (F5) was mated with BN rats and 82 backcross progeny (BCP) were produced (cross 1). To map *am*, SRR03-*am* (F6) was mated with BN rats and 98 BCP were produced (cross 2). To map *g* and *Pel*, SRR03-*g*, *Pel* (F6) was mated with BN rats and 87 BCP were produced (cross 3). To map *dmbo* and *hs*, SRR04 (F5) was mated with BN rats and 99 BCP were produced (cross 4). To map *Re*, SRR05 (F3) was mated with BN rats and 50 BCP were produced (cross 5). To map *Be*, SRR06 (F6) was mated with BN and WTC rats, and 48 and 67 BCP were produced (crosses 6 and 7).

Genotyping was performed as described previously [16] with a set of highly informative simple sequence length polymorphism (SSLP) markers [20].

Table 1. Mutations isolated from fancy rats

Mutation (symbol)	MP term (MP id)[a]	Characteristic	Origin[b]	KFRS strain	Mode of inheritance	Mapped position in rats		Candidate gene name (Gene symbol)	Mutant phenotype of candidate gene in mice
						Chr	Physical position[c]		
American mink (*am*)	diluted coat color (0000371)	Light brown body hair [26]	Unknown. Different from the original mink described by Robinson	KFRS3A/ Kyo	recessive	1	95.5–103 Mb[d]	Hermansky-Pudlak syndrom 5 (*Hps5*)	Mice Homozygous for *Hps5* mutation (*ruby-2*) have hypopigmented eyes and hair [33]
Black eye (*Be*)	diluted coat color (0000371)	Cream coat with pigmented eyes	Laboratory colony at Edinburgh University in Scotland in 1998 → Breeder in England	KFRS6/ Kyo	dominant	ND	ND		
dumbo (*dmbo*)	abnormal outer ear morphology (0002177)	Ears are set lower on the head, and are larger and rounder.	Fancy rats somewhere in the northwest US	KFRS4/ Kyo	recessive	14	79.0–84.7 Mb	H6 homeo box 1 (*Hmx1*)	Mice carrying *Hmx1* mutations exhibit enlarged ear pinnae with a distinctive ventrolateral shift [23]
grey (*g*)	diluted coat color (0000371)	Light grey body hair	Maybe Russian blue. From fancies of east coast US.	KFRS3B/ Kyo	recessive	8	57.3–95.2 Mb	RB27A, member RAS oncogene family (*Rab27a*) myosin VA (*Myo5a*)	Gene defects produce abnormal pigmentation and a gray or diluted coat color in ashen or dilute mice [22, 32] and dop rats [8].
head spot (*hs*)	head head spot (0002939)	White spotting on the head	Unknown	KFRS4/ Kyo	recessive	15	84.6–91.2 Mb	endothelin receptor type B (*Ednrb*)	Mice homozygous for the *Ednrbs* mutation show irregular white spotting, depending on the genetic background [25]
Pearle (*Pel*)	diluted coat color (0000371), embryonic lethality (0008762)	Lighter coat color expressed on mink or grey. Homozygotes die in the embryonic period (E10–E12)	English fancy [26]	KFRS3A/ Kyo KFRS3B/ Kyo	dominant	ND	ND		
Rex (*Re*)	wavy hair (0000410), nude (0003815), wavy vibrissae (0001279)	Heterozygotes show wavy body hair, while homozygotes lose body hair after the first molt. Both heterozygotes and homozygotes show wavy vibrissae.	England → Breeder in California	KFRS5/ Kyo	dominant	7	135–143 Mb[d]	keratin 71 (*Krt71*)	Mouse mutations in the *Krt71* gene, caracul (*Ca*), cause wavy coat hairs in *Ca*/+ heterozygous mice [14]
satin (*sat*)	abnormal coat appearance (0001510), curly vibrissae (0001274)	Longer hair and shiny-looking "greasy" hair. Vibrissae are bent downward.	Fancy rats kept by a breeder in California	KFRS2/ Kyo	recessive	3	105.8–114.9 Mb	fibroblast growth factor 7 (*Fgf7*)	Mice lacking the *Fgf7* gene develop a matted coat [10]
siamese (*sia*)	diluted coat color (0000371)	Homozygotes show light body hair, but their ears, nose, tail, and scrotum are dark, as in Siamese cats. Eyes are slightly pigmented and appear red.	Laboratory in France in the 1980s → Breeder in UK → breeders in California	KFRS2/ Kyo	recessive	1	140.6–145.5 Mb	tyrosinase (*Tyr*)	Mice homozygous for $Tyr^{c\text{-}h}$ show light coat color and darkened ears, nose, and scrotum. [18]

[a]: Mutant phenotypes are classified by mammalian phenotype ontology. [b]: Provided by Ms. E. Brooks. [c]: RGSC v3.4. [d]: Expected theoretical maximum distance between *am* or *Re* and non-recombinant markers. Physical distance corresponding to 1 cM was expected to be 1 Mb.

Direct sequencing of the Tyr gene of Black-eyed and Siamese rats

Direct sequencing was performed as described previously [17]. Rat *Tyr* exons were amplified with the following 6 sets of primers: rTyr-1&2 (exon 1,463 bp), 5'-TGTTTGAGCAGATCTTGTACGG-3' and 5'-TGTTTTGCCAAAGTGAGGTAA-3'; rTyr-3&11 (exon 1,633 bp) 5'-GCGGAAACTGTAAGTTTGGA-3' and 5'-AAGGTTCCTTTTCTGTGCTGA-3'; rTyr-12&13 (exon 2,398 bp), 5'-TTTCATTCATATGTAAGTCCCTTG-3' and 5'-GCTTAGCATTGCAAAACTCACA-3'; rTyr-14&15 (exon 3,384 bp), 5'-TTGTTTATTTAAAATTAGGCTTACCTC-3' and 5'-TCTCAAAATAGAGAACCACCACAA-3'; rTyr-16&17 (exon 4,488 bp), 5'-AAAGTTTGAAGATAGTCAGCATTTGA-3' and 5'-TTTAGCTGTACAAAATATCCTTGAAA-3'; rTyr-18&10 (exon 5,489 bp), 5'-GCACTCAAACCCAAGCATCT-3' and 5'-TTCCTTAGAAACTGGGACGTG-3'.

Examination of fetuses at cesarean section

Six wild-type SRR03 females (+/+) and six *Pel*-heterozygous female SRR03 (*Pel*/+) rats were mated with the *Pel*-heterozygous SRR03 males (*Pel*/+). At P20, fetuses were removed by cesarean section. The numbers of corpora lutea, live fetuses, and embryo-fetal deaths were counted. Embryo-fetal deaths were categorized into early death (implantation sites, resorbed embryos, and placental remnants) and late death (early macerated fetuses, late macerated fetuses, and dead fetuses). The number of implantations was calculated from the sum of the number of live fetuses and the number of embryo-fetal deaths.

Statistical analysis

To determine the mode of inheritance and linkage relationship, chi-square tests were performed. When the *P* value of chi-square for 1:1 was more than 0.05, the mutation was thought to be an autosomal single gene. When the *P* value of chi-square for linkage was less than 0.05, the linkage relationship between loci was thought to be significant. For statistical analysis of embryo-fetal deaths found in the Pearl mutant, Student's *t*-test was performed using Microsoft Excel.

Results

Fancy rat-derived strains

We isolated 9 mutations during inbreeding and assigned "Mammalian Phenotype terms (MP)" to their mutant phenotypes to make it easy to understand them [31] (Table 1). They involved 5 coat color mutations (*am*, *Be*, *g*, *Pel*, and *sia*), 1 coat pattern mutation (*hs*), 2 coat texture mutaions (*Re* and *sat*), and an ear pinnae malformation mutation (*dmbo*). The Pearl phenotype manifested in conjunction with homozygous status for *am* or *g*.

During inbreeding, the line originating from SRR01 became extinct. Although inbreeding was not fully completed, we tentatively named the derived lines Kyoto Fancy Rat Stock (KFRS). Each strain was defined with a number representing the names of the founder rats, and sublines were defined by the addition of a letter after the number. Six lines, including sublines, were produced and their strain names, mutations they carried, and generations at the end of February, 2010 were as follows: KFRS2/Kyo carrying *sat* and *sia* (F18), KFRS3A/Kyo carrying *am* and *Pel* (F19), KFRS3B/Kyo carrying *g* and *Pel* (F20), KFRS4/Kyo carrying *dmbo* and *hs* (F18), KFRS5A/Kyo carrying *Re* (F19), and KFRS6/Kyo carrying *Be* (F17) (Fig. 1 and Table 1).

Mode of inheritance and genetically mapped region of fancy mutations

In cross 1, 40 had satin-type body hair and 42 had normal body hair. Thirty-six had a siamese coat color, while forty-six had normal coat color. These findings indicated that both the *sat* and *sia* mutations were autosomal recessive. The linkage map including *sat* was *D3Got76* – 1.2 cM – *D3Got69*, *sat* – 1.2 cM – *D3Mco2*. The *sat* locus spanned the 9.1-Mb region defined by *D3Got76* and *D3Mco2*. The linkage map including *sia* was *D1Rat273* – 2.4 cM – *sia* – 2.4 cM – *D1Rat138*. The *sia* locus spanned the 4.9-Mb region defined by *D1Rat273* and *D1Rat138*.

In cross 2, 47 had American mink-type body hair and 51 had normal body hair, indicating the *am* mutation was autosomal recessive. The *am* showed no recombination with *D1Rat214* and *D1Mgh35* in 98 meioses, which indicated that *am* was located <3.0 cM away from these

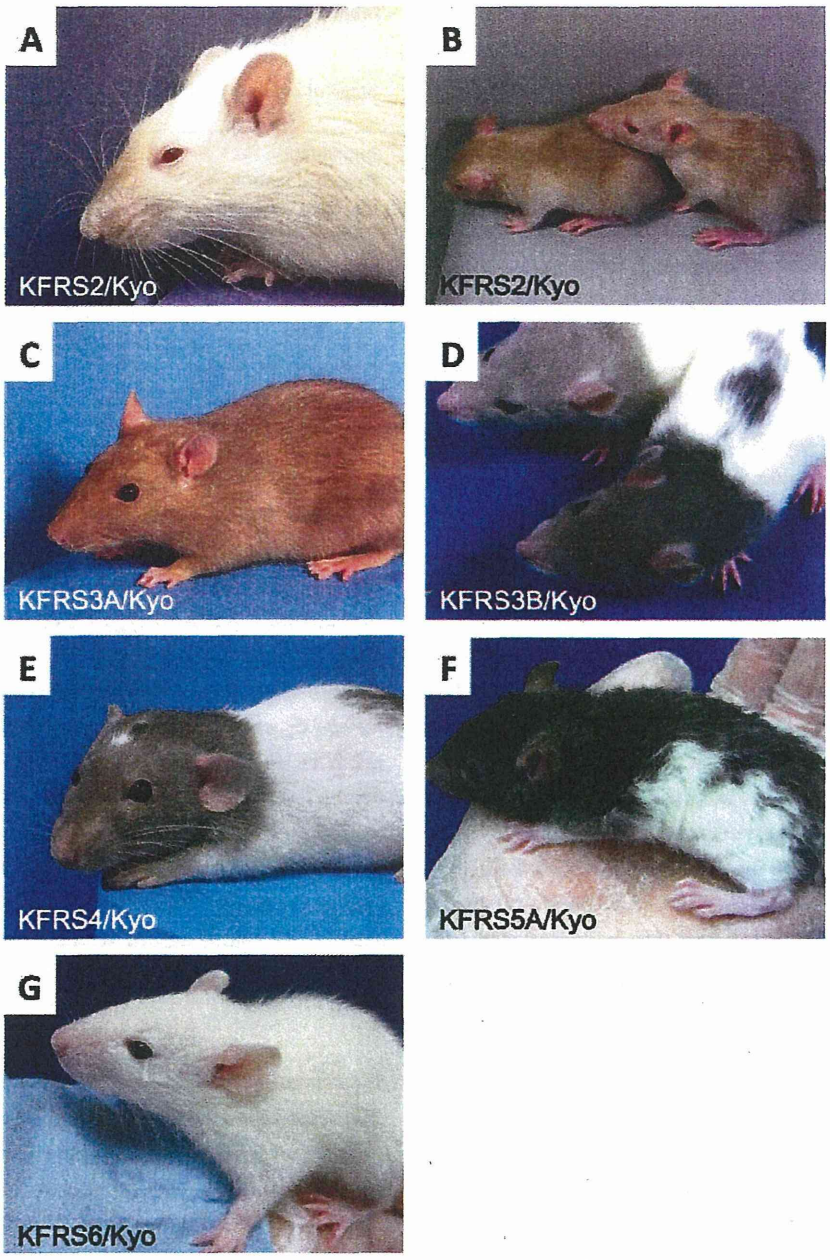

Fig. 1. Kyoto Fancy Rat Stock (KRFS) strains. (A) KFRS2/Kyo, 2 months of age, *sat/sat*, *sia/sia*. (B) KFRS2/Kyo, 3 weeks of age, Left; *sat/+*, *sia/sia*. Right; *sat/sat*, *sia/sia*. Note that siamese marking of the nose is apparent in the adult *sia/sia* rat, compared with the young rat. (C) KFRS3A/Kyo, *am/am*. (D) KFRS3B/Kyo, Upper; *g/g*, *Pel/+*. Lower; *g/g*. (E) KFRS4/Kyo, *dmbo/dmbo*, *hs/hs*. (F) KFRS5/Kyo, *Re/+*. (G) KFRS6/Kyo, *Be/Be*, *c/c*. All strains are homozygous for *a*.

markers with 95% probability [7].

In cross 3, 46 had grey-type body hair and 41 had normal body hair, indicating the *g* mutation was autosomal recessive. The linkage map including *g* was *D8Rat36* – 6.9 cM – *D8Rat182*, *g* – 14.9 cM – *D8Rat131*. The *g* locus spanned the 37.9-Mb region defined by

D8Rat36 and *D8Rat131*.

In cross 4, 55 had dumbo-type ears and 44 had normal ears. Forty-five had white spots on their head and fifty-four had no head spots. These findings indicated that both *dmbo* and *hs* mutations were autosomal recessive. The linkage map including *dmbo* was *D14Arb10* – 1.0 cM – *D14Rat37*, *dmbo* – 6.1 cM – *D14Rat57*. The *dmbo* locus spanned the 5.7-Mb region defined by *D14Rat10* and *D14Rat57*. The linkage map including *hs* was *D15Got78* – 5 cM – *hs* – 12 cM – *D15Rat26*. The *hs* locus spanned the 6.6-Mb region defined by *D15Got78* and *D15Rat26*.

In cross 5, 24 had Rex-type body hair and 26 had normal body hair, indicating that the *Re* mutation was autosomal dominant. *Re* showed no recombination with *D7Mit1* and *D7Rat80* in 50 meioses, indicating that *Re* was located <5.8 cM from these markers with 95% probability [7].

Using crosses 6 and 7, we carried out genetic analysis of the *Be* mutation. In rat fanciers, it is known that the *Be* mutation masks the coat color only in combination with the albino mutation. This combination produces rats with a pale creamy white coat color and black eyes. To elucidate the inheritance pattern of the black eye, we first crossed a SRR06 male with BN/SsNSlc (*a/a*, *b/b*, *C/C*) rats. Since all (BN/SsNSlc × SRR06)F_1 rats had a black coat and pigmented eyes, we backcrossed F_1 females to SRR06 males. In cross 6, 27 had a white coat with black eyes, and 21 had a colored coat with black eyes. The phenotype of the white coat with black eyes was completely cosegregated with a missense mutation at *Tyr*, Arg299His, found in the albino Wistar rat [4]. Direct sequencing of the *Tyr* gene of the SRR06 genome demonstrated that SRR06 also harbored the Arg299His missense mutation (data not shown).

To elucidate the inheritance pattern of the black eye on the *albino* background, we crossed a SRR06 male with albino WTC/Kyo (*a/a*, *B/B*, *c/c*) rats. All (WTC/Kyo × SRR06)F_1 rats had a white coat and black eyes. We then backcrossed the F_1 females to WTC/Kyo males. In cross 7, 29 had a white coat with black eyes, and 38 had a colored coat with black eyes. These findings indicated that the *Be* mutation was a single autosomal mutation and manifested dominantly only in the presence of the albino mutation in the homozygous state.

Table 2. Number of embryo-fetal deaths found in Pearl mutants

Stage of embryo-fetal death	Cross to produce embryos	
	+/+ × Pel/+	*Pel/+ × Pel/+*
Implantation site	0.0 ± 0.0	0.0 ± 0.0
Resorbed embryo	0.2 ± 0.4	3.0 ± 0.6**
Placental remnant	0.0 ± 0.0	0.5 ± 0.5*
Early macerated fetus	0.0 ± 0.0	0.0 ± 0.0
Late macerated fetus	0.0 ± 0.0	0.0 ± 0.0
Dead fetus	0.0 ± 0.0	0.0 ± 0.0
Total	0.2 ± 0.4	3.5 ± 0.8**

*: $P<0.05$, **: $P<0.01$.

Embryonic lethality of the Pearl (Pel) mutation

There were no significant differences in the numbers of corpora lutea [12.5 ± 1.6 vs. 12.7 ± 0.8 (mean ± SD), P=0.42] and implantations (12.2 ± 1.6 vs. 11.7 ± 0.5, P=0.25) between wild-type (+/+) and Pearl (*Pel/+*) females both crossed with Pearl (*Pel/+*) males. Meanwhile, embryo-fetus deaths were significantly higher in (*Pel/+ × Pel/+*)F_1 embryos than in (+/+ × *Pel/+*)F_1 embryos: 3.5 ± 0.8 vs. 0.2 ± 0.4, $P<0.01$ (Table 2). Embryo-fetus deaths found in (*Pel/+ × Pel/+*)F_1 embryos included resorbed embryos (3.0 ± 0.6) and placental remnant (0.5 ± 0.5). The proportion of embryo-fetus deaths with regard to the number of corpora lutea in (*Pel/+ × Pel/+*)F_1 was 27.5%, which agreed with 25% embryo-fetus death when homozygous lethality occurred in *Pel/Pel* embryos.

Identification of siamese as a missense mutation in the Tyrosinase gene

Tyrosinase (*Tyr*) was thought to be a good candidate for *sia*, because mouse *himalayan* mutation (*h*) at the *Tyr* locus showed an extremely similar coat color phenotype to the siamese rat. Direct sequencing revealed a missense mutation (c. 235 T>C, p. Ser79Pro) in exon 1 of the *tyrosinase* gene in the *sia/sia* homozygous genome (Fig. 2). This missense mutation was completely cosegragated with the siamese coat phenotype in 82 (BN × SRR02)F_1 × SRR02 BCP and was not found among 34 rat inbred strains (data not shown).

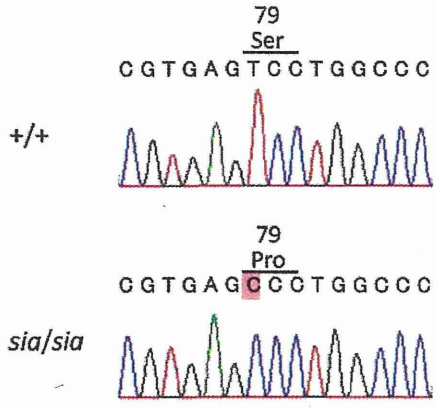

Fig. 2. Identification of siamese mutation. Sequence analysis of *Tyr* cDNA from wild-type and *sia/sia* rats. In the *sia/sia* rat, a nucleotide conversion T to C (red) was found at the position of nucleotide 253 of rat *Tyr* cDNA. The *sia* mutation converts the amino acid residue at codon 79 from serine (Ser) to proline (Pro).

Discussion

From mapped positions and phenotype resemblances to existing mutations of rats or mice, we selected candidate genes for the fancy mutations (Table 1). For *Myo5a* and *Ednrb*, rat mutations have been identified: dilute-opisthotonus (*dop*) mutation in *Myo5a* [8] and spotting lethal (*sl*) mutation in *Ednrb* [15]. We confirmed the absence of these mutations in *grey*-homozygous KFRS3B/Kyo and *head spot*-homozygous KFRS4/Kyo rats (data not shown). Therefore, all the fancy mutations isolated were likely to be unique and our study has made them available to the laboratory.

The Ser79Pro missense mutation was completely cosegregated with the siamese phenotype and was specific to KFRS2/Kyo. Missense mutations around the 79th amino acid of TYR provoke albinism in mice and humans, suggesting that this region plays an important role in hair and skin pigmentation [3, 24]. Therefore, we concluded that the S79P missense mutation is responsible for the siamese phenotype in rats. Tyrosinase is the key enzyme involved in the melanin biosynthetic pathway and is responsible for the rate limiting step [5]. Mutations in the *TYR* gene cause human oculocutaneous albinism 1 (OCA1) [24]. Although there are more than 100 mutations in the mouse *Tyr* locus, such as albino (Arg77Leu), himalayan (His420Arg), and chinchilla (Ala482Thr) [3], increasing the range of *Tyr* mutations will provide a wealth of information on the biology of tyrosinase and lead to better understanding of the pathogenesis of OCA1.

In addition to previous work on the Pearl phenotype [26], we revealed that approx. 25% embryos were largely resorbed, suggesting that *Pel/Pel* embryos die in the early stage of organogenesis (gestation days 10 to 12) [6]. There is a close relationship between *Pel* and agouti (*A*) [26]. In the current study, we carried out preliminary genetic analysis using 46 *g*-homozygous rats from cross 3. However, we failed to find a linkage relationship between *Pel* and *D3Mit2*, a SSLP marker located 2 cM apart from *A*, which suggests that multiple genetic determinants might be involved in the expression of *Pel*.

To our knowledge, this study is the first report on the systemic introduction of fancy-derived mutations to the laboratory. Fancy rats are considered to be a good source for developing a new bioresource of rats. They allow us to isolate rat mutations effectively. Usually, the rate at which new mutations arise spontaneously is exceedingly low: it is known that, on average, only one gamete in 100,000 is likely to carry a detectable mutation at any single locus naturally occurring mutation rate [28], which means that the discovery of mutations depends on chance. In this study, we could isolate 9 unique mutations from only 6 founder rats, and it took only a few generations to isolate them. Moreover, fancy rats are usually kept by outbreeding, so when they are subjected to inbreeding in the laboratory, hidden mutations sometimes manifest. Actually, we observed the cataract and sterile phenotypes, which were unknown in the SRR, at several generations after starting inbreeding (data not shown).

Fancy rat colonies are thought to be maintained relatively independent of laboratory rats and have unique breeding histories different from the laboratory rats [2]. Therefore, it is expected that the fancy-derived KFRS strains will retain their unique genetic background different from laboratory rats, although almost half of them are derived from laboratory rats. The IS/Kyo strain originates from a cross of a wild captured male rat with Wistar female rats [13] and shows a clearly different

genetic background from other strains [20]. Systematic phenotypic analysis of IS/Kyo rats uncovered their unique traits, such as hypotension and high body temperature, which implies that a wild-derived genome might confer these unique traits [19]. Following several generations, all KFRS strains will be established as full inbred strains. Thus, we consider that the systematic genotype and phenotype analyses of these KFRSs will reveal their genetic background and untapped unique traits, which make them potential disease models. Finally, phenotypically annotated KFRSs will contribute to increase the scientific value of rats.

Acknowledgments

The authors are grateful to E. Brooks for providing fancy rats, and Y. Asano and K. Katsumata for evaluating embryo-fetal deaths. KFRS2/Kyo, KFRS3A/Kyo, KFRS3B/Kyo, KFRS4/Kyo, KFRS5A/Kyo, and KFRS6/Kyo (NBRP Rat No. 0560, 0570, 0571, 0572, 0573, and 0574) are deposited in the National BioResource Project-Rat in Japan and are available from the Project (http://www.anim.med.kyoto-u.ac.jp/nbr). This work was supported in part by a Grant-in-aid for Cancer Research from the Ministry of Health, Labour and Welfare and Grants-in-aid for Scientific Research from the Japan Society for the Promotion of Science (21300153 to TK).

References

1. Aitman, T.J., Critser, J.K., Cuppen, E., Dominiczak, A., Fernandez-Suarez, X.M., Flint, J., Gauguier, D., Geurts, A.M., Gould, M., Harris, P.C., Holmdahl, R., Hubner, N., Izsvak, Z., Jacob, H.J., Kuramoto, T., Kwitek, A.E., Marrone, A., Mashimo, T., Moreno, C., Mullins, J., Mullins, L., Olsson, T., Pravenec, M., Riley, L., Saar, K., Serikawa, T., Shull, J.D., Szpirer, C., Twigger, S.N., Voigt, B., and Worley, K. 2008. Progress and prospects in rat genetics: a community view. *Nat. Genet.* 40: 516–522.
2. Baker, H.J., Lindsey, J.R., and Weisbroth, S.H. 1979. The Laboratory Rat, Academic Press, New York.
3. Beermann, F., Orlow, S.J., and Lamoreux, M.L. 2004. The Tyr (albino) locus of the laboratory mouse. *Mamm. Genome* 15: 749–758.
4. Blaszczyk, W.M., Arning, L., Hoffmann, K.P., and Epplen, J.T. 2005. A Tyrosinase missense mutation causes albinism in the Wistar rat. *Pigment Cell Res.* 18: 144–145.
5. Cooksey, C.J., Garratt, P.J., Land, E.J., Pavel, S., Ramsden, C.A., Riley, P.A., and Smit, N.P. 1997. Evidence of the indirect formation of the catecholic intermediate substrate responsible for the autoactivation kinetics of tyrosinase. *J. Biol. Chem.* 272: 26226–26235.
6. Erb, C. 2006. Embryology and teratology. pp. 817–846. *In*: The Laboratory Rat (Suckow, M.A., Weisbroth, S.H., and Franklin, C.L. eds.), Elsevier Academic Press, Burlington.
7. Friedman, J.M., Leibel, R.L., and Bahary, N. 1991. Molecular mapping of obesity genes. *Mamm. Genome* 1: 130–144.
8. Futaki, S., Takagishi, Y., Hayashi, Y., Ohmori, S., Kanou, Y., Inouye, M., Oda, S., Seo, H., Iwaikawa, Y., and Murata, Y. 2000. Identification of a novel myosin-Va mutation in an ataxic mutant rat, dilute-opisthotonus. *Mamm. Genome* 11: 649–655.
9. Gibbs, R.A., Weinstock, G.M., Metzker, M.L., Muzny, D.M., Sodergren, E.J., Scherer, S., Scott, G., Steffen, D., Worley, K.C., Burch, P.E., Okwuonu, G., Hines, S., Lewis, L., DeRamo, C., Delgado, O., Dugan-Rocha, S., Miner, G., Morgan, M., Hawes, A., Gill, R., Celera, Holt, R.A., Adams, M.D., Amanatides, P.G., Baden-Tillson, H., Barnstead, M., Chin, S., Evans, C.A., Ferriera, S., Fosler, C., Glodek, A., Gu, Z., Jennings, D., Kraft, C.L., Nguyen, T., Pfannkoch, C.M., Sitter, C., Sutton, G.G., Venter, J.C., Woodage, T., Smith, D., Lee, H.M., Gustafson, E., Cahill, P., Kana, A., Doucette-Stamm, L., Weinstock, K., Fechtel, K., Weiss, R.B., Dunn, D.M., Green, E.D., Blakesley, R.W., Bouffard, G.G., De Jong, P.J., Osoegawa, K., Zhu, B., Marra, M., Schein, J., Bosdet, I., Fjell, C., Jones, S., Krzywinski, M., Mathewson, C., Siddiqui, A., Wye, N., McPherson, J., Zhao, S., Fraser, C.M., Shetty, J., Shatsman, S., Geer, K., Chen, Y., Abramzon, S., Nierman, W.C., Havlak, P.H., Chen, R., Durbin, K.J., Egan, A., Ren, Y., Song, X.Z., Li, B., Liu, Y., Qin, X., Cawley, S., Worley, K.C., Cooney, A.J., D'Souza, L.M., Martin, K., Wu, J.Q., Gonzalez-Garay, M.L., Jackson, A.R., Kalafus, K.J., McLeod, M.P., Milosavljevic, A., Virk, D., Volkov, A., Wheeler, D.A., Zhang, Z., Bailey, J.A., Eichler, E.E., Tuzun, E., Birney, E., Mongin, E., Ureta-Vidal, A., Woodwark, C., Zdobnov, E., Bork, P., Suyama, M., Torrents, D., Alexandersson, M., Trask, B.J., Young, J.M., Huang, H., Wang, H., Xing, H., Daniels, S., Gietzen, D., Schmidt, J., Stevens, K., Vitt, U., Wingrove, J., Camara, F., Mar Alba, M., Abril, J.F., Guigo, R., Smit, A., Dubchak, I., Rubin, E.M., Couronne, O., Poliakov, A., Hubner, N., Ganten, D., Goesele, C., Hummel, O., Kreitler, T., Lee, Y.A., Monti, J., Schulz, H., Zimdahl, H., Himmelbauer, H., Lehrach, H., Jacob, H.J., Bromberg, S., Gullings-Handley, J., Jensen-Seaman, M.I., Kwitek, A.E., Lazar, J., Pasko, D., Tonellato, P.J., Twigger, S., Ponting, C.P., Duarte, J.M., Rice, S., Goodstadt, L., Beatson, S.A., Emes, R.D., Winter, E.E., Webber, C., Brandt, P., Nyakatura, G., Adetobi, M., Chiaromonte, F., Elnitski, L., Eswara, P., Hardison, R.C., Hou, M., Kolbe, D., Makova, K., Miller, W., Nekrutenko, A., Riemer, C., Schwartz, S., Taylor, J., Yang, S., Zhang, Y., Lindpaintner, K., Andrews, T.D., Caccamo, M., Clamp, M., Clarke, L., Curwen, V., Durbin, R., Eyras, E., Searle, S.M., Cooper, G.M., Batzoglou, S., Brudno, M., Sidow, A., Stone, E.A., Venter, J.C., Payseur, B.A., Bourque, G., Lopez-Otin, C., Puente, X.S., Chakrabarti, K., Chatterji, S., Dewey, C.,

Pachter, L., Bray, N., Yap, V.B., Caspi, A., Tesler, G., Pevzner, P.A., Haussler, D., Roskin, K.M., Baertsch, R., Clawson, H., Furey, T.S., Hinrichs, A.S., Karolchik, D., Kent, W.J., Rosenbloom, K.R., Trumbower, H., Weirauch, M., Cooper, D.N., Stenson, P.D., Ma, B., Brent, M., Arumugam, M., Shteynberg, D., Copley, R.R., Taylor, M.S., Riethman, H., Mudunuri, U., Peterson, J., Guyer, M., Felsenfeld, A., Old, S., Mockrin, S., and Collins, F. 2004. Genome sequence of the Brown Norway rat yields insights into mammalian evolution. *Nature* 428: 493–521.

10. Guo, L., Degenstein, L., and Fuchs, E. 1996. Keratinocyte growth factor is required for hair development but not for wound healing. *Genes Dev.* 10: 165–175.
11. Hedrich, H.J. 2006. Taxonomy and stocks and strains. pp. 71–92. *In*: The Laboratory Rat (Suckow, M.A., Weisbroth, S.H., and Franklin, C.L. eds.), Elsevier Academic Press, Burlington.
12. Ibrahim, N. and Haluska, F.G. 2009. Molecular pathogenesis of cutaneous melanocytic neoplasms. *Annu. Rev. Pathol.* 4: 551–579.
13. Ishibashi, M. 1979. [History and summary of Ishibashi rats (ISR)]. *Jikken Dobutsu* 28: 599–600 (in Japanese).
14. Kikkawa, Y., Oyama, A., Ishii, R., Miura, I., Amano, T., Ishii, Y., Yoshikawa, Y., Masuya, H., Wakana, S., Shiroishi, T., Taya, C., and Yonekawa, H. 2003. A small deletion hotspot in the type II keratin gene mK6irs1/Krt2-6g on mouse chromosome 15, a candidate for causing the wavy hair of the caracul (*Ca*) mutation. *Genetics* 165: 721–733.
15. Kunieda, T., Kumagai, T., Tsuji, T., Ozaki, T., Karaki, H., and Ikadai, H. 1996. A mutation in endothelin-B receptor gene causes myenteric aganglionosis and coat color spotting in rats. *DNA Res.* 3: 101–105.
16. Kuramoto, T., Kitada, K., Inui, T., Sasaki, Y., Ito, K., Hase, T., Kawagachi, S., Ogawa, Y., Nakao, K., Barsh, G.S., Nagao, M., Ushijima, T., and Serikawa, T. 2001. Attractin/mahogany/zitter plays a critical role in myelination of the central nervous system. *Proc. Natl. Acad. Sci. U.S.A.* 98: 559–564.
17. Kuramoto, T., Kuwamura, M., and Serikawa, T. 2004. Rat neurological mutations *cerebellar vermis defect* and *hobble* are caused by mutations in the netrin-1 receptor gene *Unc5h3*. *Brain Res. Mol. Brain Res.* 122: 103–108.
18. Kwon, B.S., Halaban, R., and Chintamaneni, C. 1989. Molecular basis of mouse Himalayan mutation. *Biochem. Biophys. Res. Commun.* 161: 252–260.
19. Mashimo, T., Voigt, B., Kuramoto, T., and Serikawa, T. 2005. Rat Phenome Project: the untapped potential of existing rat strains. *J. Appl. Physiol.* 98: 371–379.
20. Mashimo, T., Voigt, B., Tsurumi, T., Naoi, K., Nakanishi, S., Yamasaki, K., Kuramoto, T., and Serikawa, T. 2006. A set of highly informative rat simple sequence length polymorphism (SSLP) markers and genetically defined rat strains. *BMC Genet.* 7: 19.
21. Mashimo, T., Yanagihara, K., Tokuda, S., Voigt, B., Takizawa, A., Nakajima, R., Kato, M., Hirabayashi, M., Kuramoto, T., and Serikawa, T. 2008. An ENU-induced mutant archive for gene targeting in rats. *Nat. Genet.* 40: 514–515.
22. Mercer, J.A., Seperack, P.K., Strobel, M.C., Copeland, N.G., and Jenkins, N.A. 1991. Novel myosin heavy chain encoded by murine dilute coat colour locus. *Nature* 349: 709–713.
23. Munroe, R.J., Prabhu, V., Acland, G.M., Johnson, K.R., Harris, B.S., O'Brien, T.P., Welsh, I.C., Noden, D.M., and Schimenti, J.C. 2009. Mouse H6 Homeobox 1 (*Hmx1*) mutations cause cranial abnormalities and reduced body mass. *BMC Dev. Biol.* 9: 27.
24. Oetting, W.S. 2000. The tyrosinase gene and oculocutaneous albinism type 1 (OCA1): a model for understanding the molecular biology of melanin formation. *Pigment Cell Res.* 13: 320–325.
25. Pavan, W.J., Mac, S., Cheng, M., and Tilghman, S.M. 1995. Quantitative trait loci that modify the severity of spotting in piebald mice. *Genome Res.* 5: 29–41.
26. Robinson, R. 1994. Mink and pearl: new color mutants in the Norway rat. *J. Hered.* 85: 142–143.
27. Serikawa, T., Mashimo, T., Takizawa, A., Okajima, R., Maedomari, N., Kumafuji, K., Takami, F., Neoda, Y., Otsuki, M., Nakanishi, S., Yamasaki, K., Voigt, B., and Kuramoto, T. 2009. National BioResource Project-Rat and related activities. *Exp. Anim.* 58: 333–341.
28. Silver, L.M. 1995. Mouse Genetics: Concepts and Applications, Oxford University Press, New York.
29. Spritz, R.A. 1997. Piebaldism, Waardenburg syndrome, and related disorders of melanocyte development. *Semin. Cutan. Med. Surg.* 16: 15–23.
30. Steel, K.P. 1995. Inherited hearing defects in mice. *Annu. Rev. Genet.* 29: 675–701.
31. The Jackson Laboratory, Bar Harbor, Maine. Mammalian Phenotype (MP) Browser at the Mouse Genome Informatics website. [Online] http://www.informatics.jax.org/searches/MP_form.shtml. (August, 2009).
32. Wilson, S.M., Yip, R., Swing, D.A., O'Sullivan, T.N., Zhang, Y., Novak, E.K., Swank, R.T., Russell, L.B., Copeland, N.G., and Jenkins, N.A. 2000. A mutation in *Rab27a* causes the vesicle transport defects observed in ashen mice. *Proc. Natl. Acad. Sci. U.S.A.* 97: 7933–7938.
33. Zhang, Q., Zhao, B., Li, W., Oiso, N., Novak, E.K., Rusiniak, M.E., Gautam, R., Chintala, S., O'Brien, E.P., Zhang, Y., Roe, B.A., Elliott, R.W., Eicher, E.M., Liang, P., Kratz, C., Legius, E., Spritz, R.A., O'Sullivan, T.N., Copeland, N.G., Jenkins, N.A., and Swank, R.T. 2003. *Ru2* and *Ru* encode mouse orthologs of the genes mutated in human Hermansky-Pudlak syndrome types 5 and 6. *Nat. Genet.* 33: 145–153.

ROLE OF POLY-ADP-RIBOSYLATION IN THE MAINTENANCE OF GENOMIC STABILITY

Mitsuko Masutani, Hidenori Shirai, Hideki Ogino, Anna Poetsch, Erika Sasamoto, Daisuke Maeda, Aki Hashimoto and Takashi Sugimura

Biochemistry Division

National Cancer Center Research Institute

1-1, Tsukiji, 5-chome, Chuo-ku, Tokyo 104-0045, Japan

(mmasutan@ncc.go.jp)

Poly-ADP-ribosylation is a unique post-translational modification catalyzed by poly(ADP-ribose) polymerase (PARP) using β-NAD^+ as a substrate. PARP-1 is activated by DNA strand breaks and is involved in DNA repair pathways, including base excision repair (BER) and single and double strand break repairs. PARP-1 is also involved in the regulation of transcription and chromatin function. Poly(ADP-ribose) is degraded mainly by poly(ADP-ribose) glycohydrolase (PARG) to ADP-ribose in the cells.

We have investigated the role of PARP-1 and PARG in the maintenance of genomic stability and carcinogenesis. *Parp-1*$^{-/-}$ mice[1] showed increased incidence of tumors induced by alkylating agents, including *N*-nitrosobis (2-hydroxypropyl) amine (BHP)[2]. No increase in the incidence was observed in the case with 4-nitroquinoline 1-oxide (4NQO)[3]. This susceptibility difference may reflect the active involvement of PARP-1 in BER and strand break repair working after alkylation damage on DNA but not nucleotide excision repair, which targets bulky DNA adducts induced by 4NQO.

The frequencies of both simple and complex-type deletion mutations, but not base substitution mutations, were augmented in the livers of *Parp-1*$^{-/-}$ compared to *Parp-1*$^{+/+}$ mice after BHP treatment[4]. *Parp-1* deficiency also caused an increase of deletion mutations in the liver at an advanced age[5]. PARP-1 is thus involved in suppressing imprecise repair of DNA damage leading to deletion mutation. This role of PARP-1 was further confirmed by a cell-free repair assay system of double strand breaks.

On the other hand, when we analyzed mutations in *Parp-1*$^{+/+}$ and *Parp-1*$^{-/-}$ mice 3 days after γ-irradiation at 8 Gy, the frequencies of deletion mutation were increased 3-fold in *Parp-1*$^{+/+}$ mice by γ-irradiation, whereas the those in *Parp-1*$^{-/-}$ mice were not increased as in

the case of knockout mice defective in end-joining repair.

Specific and potent PARP inhibitors have been developed and are now in clinical trials of cancers. Because *Parp-1*$^{-/-}$ mice showed increased susceptibility to tumor induction by alkylating agents[2,6] and higher frequencies of deletion mutations and other genomic instabilities[3,7], there is a possibility that the long-term effect of PARP inhibitors on genomic instability and cancer risk could be a potential problem in therapeutic use.

Parg$^{-/-}$ mouse ES cell lines, established by disrupting both alleles of *Parg* exon 1, exhibited enhanced lethality after γ-irradiation, treatment with cisplatin[8] and methylmethanesulfonate (MMS) compared with wild-type ES cells. After MMS treatment, early events were enhanced, such as accumulation of poly(ADP-ribose), p53 network activation, NAD depletion, γH2AX foci formation and S-phase arrest in *Parg*$^{-/-}$ ES cells. Later, the cell death processes, including caspase activation, and DNA fragmentation, were augmented. These results suggest the possibility that PARG is also involved in DNA damage response and functional inhibition of PARG possibly leads to sensitization of tumor cells to chemo- and radiation therapies. There are only a few PARG inhibitors available and the development of new specific PARG inhibitors is expected.

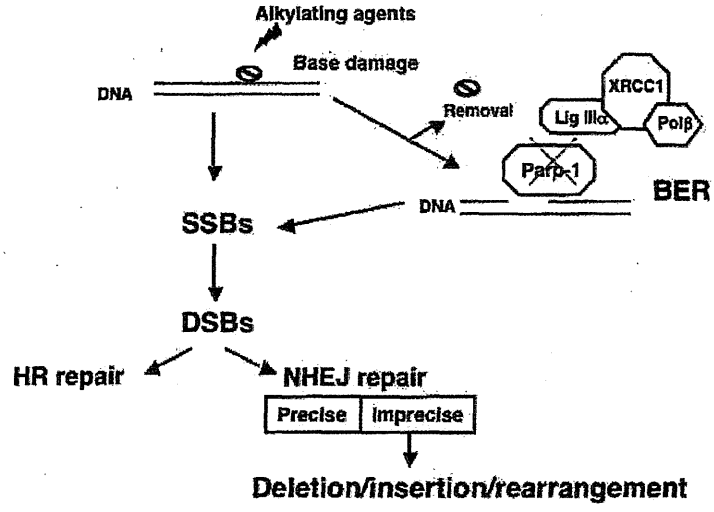

Figure 1 Model for DNA repair response under *Parp-1* deficiency.

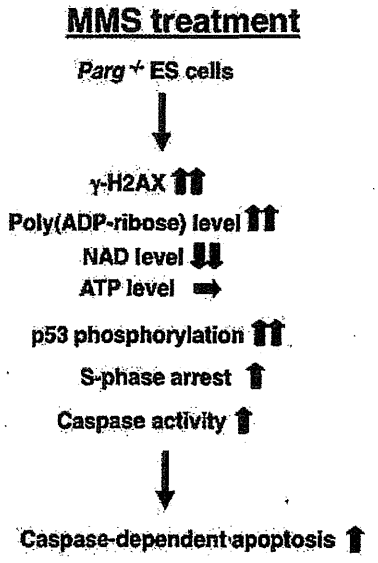

Figure 2 Enhanced lethality after MMS treatment in *Parg*$^{-/-}$ ES cells.

References

1. Masutani M, Suzuki H, Kamada N, Watanabe M, Ueda O, Nozaki T, Jishage K, Watanabe T, Sugimoto T, Nakagama H, Ochiya T, Sugimura T. Poly(ADP-ribose) polymerase gene disruption conferred mice resistant to streptozotocin-induced diabetes. Proc. Natl. Acad. Sci. USA, 96: pp.2301-2304, 1999
2. Tsutsumi M, Masutani M, Nozaki T, Kusuoka O, Tsujiuchi T, Nakagama H, Suzuki H, Konishi Y, Sugimura T. Increased susceptibility of poly(ADP-ribose) polymerase-1 knockout mice to nitrosamine carcinogenicity. Carcinogenesis, 22: pp.1-3, 2001
3. Gunji A, Uemura A, Tsutsumi M, Nozaki T, Kusuoka O, Omura K, Suzuki H, Nakagama H, Sugimura T, Masutani M. *Parp-1* deficiency does not increase the frequency of tumors in the oral cavity and esophagus of ICR/129Sv mice by 4-nitroquinoline 1-oxide, a carcinogen producing bulky adducts. Cancer Lett., 241:pp.87-92, 2006
4. Shibata A, Kamada N, Masumura K, Nohmi T, Kobayashi S, Teraoka H, Nakagama H, Sugimura T, Suzuki H, Masutani M. *Parp-1* deficiency causes an increase of deletion mutations and insertions/rearrangements *in vivo* after treatment with an alkylating agent. Oncogene, 24: pp.1328-1337, 2005

5. Shibata A, Maeda D, Ogino H, Tsutsumi M, Nohmi T, Nakagama H, Sugimura T, Teraoka H, Masutani M. Role of Parp-1 in suppressing spontaneous deletion mutation in the liver and brain of mice at adolescence and advanced age. Mutat. Res./Fundamental and Molecular Mechanisms of Mutagenesis, 664: pp.20-27, 2009
6. Nozaki T, Fujihara H, Watanabe M, Tsutsumi M, Nakamoto K, Kusuoka, O, Kamada N, Suzuki H, Nakagama H, Sugimura T, Masutani M. *Parp-1* deficiency implicated in colon and liver tumorigenesis induced by azoxymethane. Cancer Sci., 94:pp.497-500, 2003
7. de Murcia JM, Niedergang C, Trucco C, Ricoul M, Dutrillaux B, Mark M, Oliver FJ, Masson M, Dierich A, LeMeur M, Walztinger, C, Chambon, P, de Murcia, G. Requirement of poly(ADP-ribose) polymerase in recovery from DNA damage in mice and in cells. Proc Natl Acad Sci USA, 94: pp.7303-7307, 1997
8. Fujihara H, Ogino H, Maeda D, Shirai H, Nozaki T, Kamada N, Jishage K, Tanuma S, Takato T, Ochiya T, Sugimura T, Masutani M. Poly(ADP-ribose) glycohydrolase deficiency sensitizes mouse ES cells to DNA damaging agents. Current Cancer Drug Targets, In press.

Dr. Mitsuko Masutani, Ph.D.

1985	MS, Okayama University
1988	Ph.D., University of Tokyo
1988-1989	Research Fellow, JSPS, University of Tokyo
1989-1992	Research Resident Fellow, National Cancer Center Research Institute (NCCRI)
1992-1997	Research Staff, Biochemistry Division, NCCRI
1997-2007	Section Head, Biochemistry Division, NCCRI
2005-2008	Project Leader, ADP-ribosylation in Oncology Project NCCRI
2007-	Chief, Biochemistry Division, NCCRI

Specialty and Present Interest:
Poly-ADP-ribosylation, Biochemistry, Carcinogenesis, Cancer Prevention and Treatment

OPEN ACCESS Freely available online

PLoS one

PolyADP-Ribosylation Is Required for Pronuclear Fusion during Postfertilization in Mice

Tomoharu Osada[1,2]*, Hideki Ogino[3,4], Toshiaki Hino[5], Sachiyo Ichinose[6], Kenji Nakamura[5], Akira Omori[6], Toshiaki Noce[2], Mitsuko Masutani[3,4]*

1 Advanced Medical Science Research Center, Mitsubishi Chemical Medience Corporation, Minato-ku, Tokyo, Japan, **2** Department of Regenerative and Developmental Biology, Mitsubishi Kagaku Institute of Life Sciences (MITILS), Machida, Tokyo, Japan, **3** Biochemistry Division, National Cancer Research Institute, Chuo-ku, Tokyo, Japan, **4** ADP-ribosylation in Oncology Project, National Cancer Research Institute, Chuo-ku, Tokyo, Japan, **5** Mouse Genome Technology Laboratory, Mitsubishi Kagaku Institute for Life Sciences (MITILS), Machida, Tokyo, Japan, **6** Bio-molecular Structure Analysis Laboratory, Mitsubishi Kagaku Institute for Life Sciences (MITILS), Machida, Tokyo, Japan

Abstract

Background: During fertilization, pronuclear envelope breakdown (PNEB) is followed by the mingling of male and female genomes. Dynamic chromatin and protein rearrangements require posttranslational modification (PTM) for the postfertilization development.

Methodology/Principal Findings: Inhibition of poly(ADP-ribose) polymerase activity (PARylation) by either PJ-34 or 5-AIQ resulted in developmental arrest of fertilized embryos at the PNEB. PARylation inhibition affects spindle bundle formation and phosphorylation of Erk molecules of metaphase II (MII) unfertilized oocytes. We found a frequent appearance of multiple pronuclei (PN) in the PARylation-inhibited embryos, suggesting defective polymerization of tubulins. Attenuated phosphorylation of lamin A/C by PARylation was detected in the PARylation-inhibited embryos at PNEB. This was associated with sustained localization of heterodomain protein 1 (HP1) at the PN of the one-cell embryos arrested by PARylation inhibition.

Conclusions/Significance: Our findings indicate that PARylation is required for pronuclear fusion during postfertilization processes. These data further suggest that PARylation regulates protein dynamics essential for the beginning of mouse zygotic development. PARylation and its involving signal-pathways may represent potential targets as contraceptives.

Citation: Osada T, Ogino H, Hino T, Ichinose S, Nakamura K, et al. (2010) PolyADP-Ribosylation Is Required for Pronuclear Fusion during Postfertilization in Mice. PLoS ONE 5(9): e12526. doi:10.1371/journal.pone.0012526

Editor: Hongmei Wang, Institute of Zoology, Chinese Academy of Sciences, China

Received March 19, 2010; **Accepted** July 27, 2010; **Published** September 2, 2010

Funding: This work is supported in part by Grant-in-Aid from the Ministry of Education, Science, Sports, and Culture of Japan (T.O., 18870035) (http://www.mext.go.jp), Grant-in-Aid for the Third Term Comprehensive 10-year Strategy for Cancer Control (M.M., H19-Sanjigan-Ippan-003) and Grant-in-Aid from the Ministry of Health, Labour and Welfare of Japan (M.M.) (http://www.mhlw.go.jp). The funders had no role in study design, data collection and analysis, decision to publish, or preparation of the manuscript.

Competing Interests: The authors have declared that no competing interests exist.

* E-mail: osada.tomoharu@mg.medience.co.jp (TO); mmasutan@ncc.go.jp (MM)

Introduction

Fertilization comprises a series of biological steps beginning with the recognition between the egg and sperm cells and ending at the mingling of genetic materials of these two cells [1]. Previous studies have elucidated the behavior of various cell organelles and proteins within the egg during fertilization [2]. In humans, arrest of fertilized eggs at the pronuclear (PN) stage is commonly observed after *in vitro* fertilization (IVF) or intracytoplasmic sperm injection (ICSI) [3]. We know little about the molecular mechanisms of the pronuclear envelope breakdown (PNEB) and the mingling of male and female genomes. Since zygotic genes are largely expressed only after the first cleavage of embryos [4], it is most likely that the posttranslational modification (PTM) of maternal proteins plays central regulatory roles before and during the PNEB.

A wealth of study has reported the dynamic PTMs of nuclear proteins during the first cell-cycle of mouse development. Phosphorylation transmits intracellular signals into nuclear proteins, which mainly drives progression of the first cell-cycle [5]. Like in carcinogenesis and other cellular processes, chromatin modification systems including histone acetylation and methylation in early embryos are involved in the gene expression regulation mediated by remodeling of chromatin structure [6]. Chromatin modifications are different between parental chromatins at the one-cell embryo [7]. Although biological significance of the PTM is elusive during postfertilization development, it is acceptable that the maternal PTM would regulate zygotic gene activation at the 2-cell stage embryos [8].

To understand the molecular machinery essential for the postfertilization events, we studied the effects of reagents that affect poly(ADP-ribosylation) (PARylation). Poly(ADP-ribose) polymerase (Parp) is known to contribute to DNA repair, transcription, and spindle assembly by transferring negatively charged poly(ADP-ribose) polymers (PAR) to acceptor proteins [9,10]. While the mice lacking Parp1, the most abundant PARP, are viable and fertile [11], those lacking both Parp1 and Parp 2 die at the onset of gastrulation [12]. PARylation is also regulated by

poly(ADP-ribose) glycohydrolase (Parg), which cleaves ribosyl-ribose linkages of ADP-ribose polymer. Mice lacking the *Parg* gene are lethal during cleavage-stage of mouse embryogenesis, with accumulation of ADP-ribose polymers [13]. These data suggest that the PARylation contributes to the early stages of mouse embryogenesis. Recent studies elucidated that PARylation system is regulated by Parp family genes, 17 of which have been identified so far [10]. We addressed the role of total PARylation reactions catalyzed by members of Parp family during fertilization process, utilizing PARP inhibitors. In the case of Parp knockout animals, we are not able to avoid compensatory effects of other Parp family members. The use of PARP inhibitors could enable us to examine the effects of blocking whole PARylation reactions. These data will elucidate biological windows for the dissection of the complex PARylation system during mouse embryogenesis.

Results

Levels of Parp1, ADP-ribose polymer, Parg, and Parp-family gene expression in MII oocytes and postfertilized embryogenesis

To assess the presence and activation of PARylation system in oocytes, we first examined the localization of Parp1 and poly(ADP-ribose) (PAR) in the MII oocytes and one-cell embryos. Immunoreactivity on meiotic spindles of MII oocytes was detected for Parp1, but not for PAR (Figure 1A, D). Upon fertilization, signals on meiotic spindles were detected for both Parp1 and PAR (Figure 1B, E). Six hours after IVF, pronuclear staining was observed for both Parp1 and PAR (Figure 1C, F). We next analyzed Parg activity by measuring the release of ADP-ribose from PAR as substrates in the extracts prepared from MII oocytes, Sr^{2+}-activated parthenogenetic embryos and IVF one-cell embryos (Figure 1G). The Parg activity was detected in all of the above, indicating that Parg also regulates PARylation in unfertilized and postfertilized (activated) eggs. The RT-PCR analyses exhibited that 12 of 17 *Parp* family and the *Parg* genes were detectable (Figure 1H).

Developmental arrest of PJ-34 treated embryos at the pronuclear fusion during postfertilization development

We next performed IVF to examine the significance of PARylation in postfertilization period (Table 1, Figure 2A). Effects of PARylation inhibition were assessed with 4 different protocols (Figure 2A). In Exp. 1, no Parp inhibitor was added. In Exp. 2, Parp inhibitors were added 1 hour before IVF or ICSI, subsequently incubated for 6 hrs, and then embryos were transferred in the new culture media without Parp inhibitors. In Exp. 3, Parp inhibitors were added 6 hrs after IVF or ICSI. In Exp. 4, Parp inhibitors were added 1 hr before IVF or ICSI and were present throughout the experiments. PJ-34 [14] and 5-

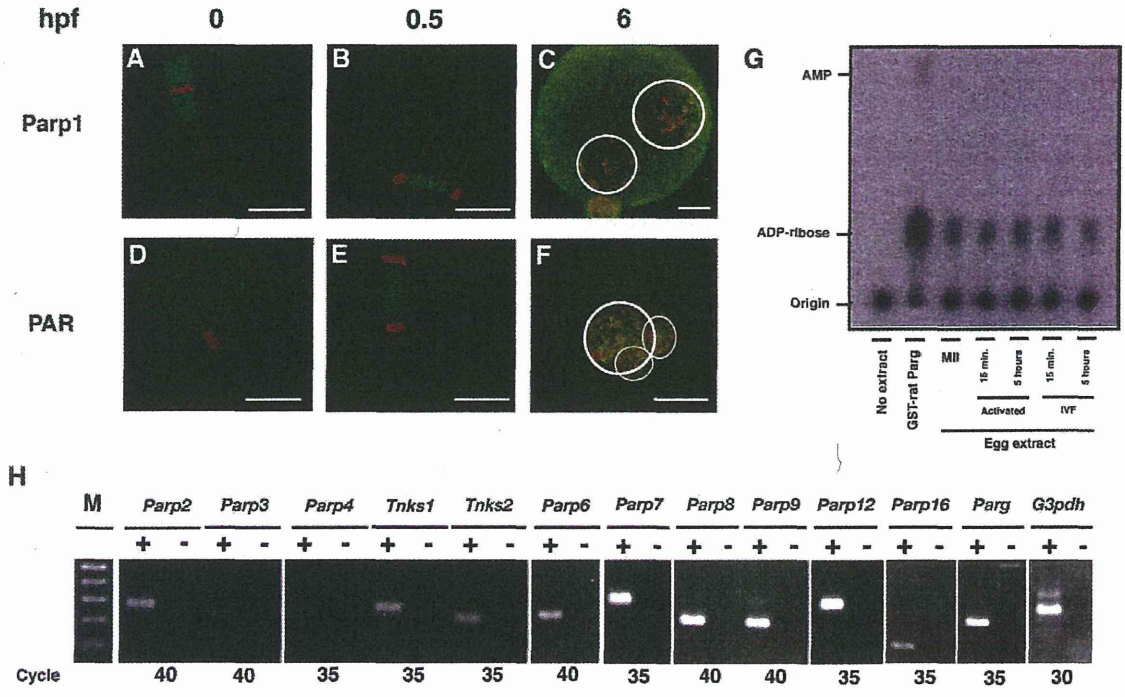

Figure 1. Expression of Parp, PAR level and Parg activity in the mouse oocytes. Immunofluorescence analyses of MII oocytes (**A, D**), embryos at 0.5 hpf (**B, E**) and 6 hpf (**C, F**) with antibody for Parp1 (**A–C**) and PAR (**D–F**). Detected antigens were colored with green. DNA was counterstained with PI, colored in red. White circles represent the outlines of pronuclei (PNs). Bars indicate 20 μm. (**G**) Thin layer chromatography (TLC) for the detection of poly(ADP-ribose) glycohydrolase (Parg) activity. Purified GST-Parg proteins and crude extracts from MII oocytes, parthenogenetic (activated) and untreated (IVF) embryos at 15 min and 5 hrs after activation/fertilization were loaded and reacted with synthetic PAR polymers. Release of ADP-ribose was detected by the mobility of spots from origin. A spot with high-mobility in the GST-rat Parg-loaded lane represents adenosine monophosphate (AMP). (**H**) RT-PCR analyses with primer sets for the 12 *Parp*-family genes, the *Parg* gene, and glyceraldehyde-3-phosphatase dehydrogenase (*G3pdh*) gene. Amplified DNA with cDNA synthesized with reverse transcriptase (+) or without enzymes (−) was loaded in each lane. PCR reaction was carried out with the number of cycles indicated. The 100-bp ladder marker DNA was shown (M). The lowest DNA band corresponds to the 100 base pair (bp).
doi:10.1371/journal.pone.0012526.g001

Table 1. Postfertilization development of untreated and PARP inhibitor-treated mouse embryos.

Test	Exp.*	Chemicals	Dose (μM)	No. oocytes examined	No. of embryos developed to 2-cell (%)**	Blastcyst (%)**
IVF	1	untreated	0	258	245 (100)[a]	224 (96.1)
	2	PJ-34	30	174	161 (95.8)	134 (93.3)
		5-AIQ	20	63	58 (99)	41 (92.1)
	3	PJ-34	30	126	4 (3.2)[a]	0 (0)[a]
		5-AIQ	20	71	3 (4.2)[a]	0 (0)[a]
	4	PJ-34	30	189	0 (0)[a]	0 (0)[a]
		5-AIQ	20	78	0 (0)[a]	0 (0)[a]
ICSI	1	untreated	0	118	103 (87.3)	94 (79.7)
	2	PJ-34	6	86	67 (77.9)	62 (72.1)
		5-AIQ	30	74	26 (35.1)[b]	22 (29.7)[b]
	3	PJ-34	6	67	11 (16.4)[a]	3 (4.5)
		5-AIQ	30	64	0 (0)[a]	0 (0)[a]
	4	PJ-34	6	102	7 (6.9)[a]	6 (5.9)[a]
		5-AIQ	30	104	0 (0)[a]	0 (0)[a]

*PJ-34 or 5-AIQ was added 1 hr before IVF or ICSI and removed 6 hrs later (Exp. 2), added 6 hrs after IVF or ICSI (Exp. 3), and added 1 hr before IVF or ICSI and continuously treated for subsequent 24 hrs (Exp. 4). Inhibitors were included in the medium at the designated doses and the developmental effects were shown. Both PJ-34 and 5-AIQ were used for IVF and PJ-34 was used for ICSI. Development of untreated embryos was assessed as positive control (Exp. 1). Each experimental procedure was illustrated in Figure 2A.

**Percentage is calculated by the formula: $(\%) = \frac{\text{Number of embryos developed.}}{\text{Number of oocytes examined.}} \times 100.$

[a, b]Statistic significance is compared with number of untreated oocytes or embryos by t-test ($p<0.01$ (a), $p<0.05$ (b)).

doi:10.1371/journal.pone.0012526.t001

aminoisoquinolinone (5-AIQ) [15] were used as PARylation inhibitors in this study. IC_{50} of PJ-34 for PARP-1 activity is 20 nM [14]. In normal or cancer cells, inhibitory effect of PJ-34 on PARylation is usually assessed at around 3-10 μM, for example, in A549 cells [16], and cardiac fibroblasts [17]. On the other hand, the effects of PARylation inhibition are also assessed at 30 μM PJ-34 in macrophages [18], T cells [19], neurons [20], or human breast cancer cells MCF-7, and MDA231 [21]. The permeability of the oocyte membrane is unique, and many investigations have been carried out at different concentrations of chemicals compared to the cases of cell lines *in vitro*. 3-AB was used at 5 mM as a Parp inhibitor for oocyte treatment, which has IC_{50} value for PARP-1 activity around 30 μM [22]. Based on this information we used a concentration of 30 μM PJ-34 for treatment of oocytes in this study. The first mitotic cleavage was not completed when the IVF embryos were incubated with 30 μM PJ-34 (0/189 (0%)) or 20 μM 5-AIQ (0/78 (0%), Exp. 4) (Table 1). Transition beyond the 2-cell embryos was slightly perturbed when incubated with 6 μM PJ-34 (86/90 (95.6%)) or 4 μM 5-AIQ (64/78 (82.1%)) (data not shown). The lower frequency of development to 2-cell embryos was observed when the embryos were incubated for 18 hrs from 6 hrs after IVF with 30 μM PJ-34 (4/126 (3%)) and 20 μM 5-AIQ (3/71 (4.2%), Exp. 3). We also performed intracytoplasmic injection (ICSI) experiment to omit the possible damage on sperm DNA by the PARylation inhibitors in the culture medium. Development to 2-cell embryos was stopped when the ICSI embryos were incubated for 25 hrs with either 30 μM PJ-34 (0/104 (0%)) or 6 μM PJ-34 (7/102 (7%), Exp. 4). The frequency of developmental arrest was higher in the ICSI embryos treated with 30 μM PJ-34 from 6 hrs after injection of sperm into oocytes (0/63 (0%), Exp. 3), than embryos treated with PJ-34 for 6 hrs after injection of sperm into oocytes (26/74 (35%), Exp. 2). These data indicate that PARylation inhibition results in developmental arrest of the first mitotic cleavage in mice. Experiments with PARylation inhibitors suggest that PARylation is more important for the late PN stage of mouse embryogenesis. ICSI experiments suggest that developmental defects by PARylation inhibition are mainly due to the effects on maternal genetic materials or proteins.

We observed a vast majority of non-treated one-cell embryos 36 hrs after IVF progressed to the first mitotic cleavage (Figure 2B), whereas PARylation-inhibited embryos stopped at the pronuclear envelope breakdown (PNEB) (Figure 2C, D). Further analyses evaluated the cell cycle progression of PARylation-inhibited embryos by immunofluorescence. BrdU incorporation (Figure 2M–P) and phosphorylation of histone H3 at serine 10, which is known as a G2 phase and mitotic marker, were detected in the both pronuclei (PNs) of one cell embryos untreated or treated with 30 μM PJ-34 or 20 μM 5-AIQ 10 hrs after IVF (Figure 2E–L). These data indicate that DNA synthesis and progression to G2 phase are occurred in both untreated or PARylation inhibited PNs.

Male PNs were preferentially stained with the phosphorylated histone H3 antibody by PARylation inhibition, which may be due to the accelerated S-phase progression of male PNs. However, there is another possibility that the increased content of histone H3 in male PNs compared to female PNs by PARylation inhibition could cause the differential staining with phosphorylated histone H3 antibody. Further analysis should elucidate the detailed roles of PARylation in the replication timing in PNs. These data suggest that PARylation is required for PNEB, but DNA synthesis and cell-cycle progression to G2 phase are not largely affected by PARylation inhibitor.

Spindle modification by PARylation in MII oocytes and postfertilization development

To explore the cause of developmental arrest by PARylation inhibition, we first focused on spindle formation, because Parp1 signals were predominantly localized to the meiotic spindles and